

The impact of SiN_x gate insulators on amorphous indium-gallium-zinc oxide thin film transistors under bias-temperature-illumination stress

Ji Sim Jung,¹ Kyoung Seok Son,¹ Kwang-Hee Lee,¹ Joon Seok Park,¹ Tae Sang Kim,¹ Jang-Yeon Kwon,^{1,a)} Kwun-Bum Chung,² Jin-Seong Park,^{3,a)} Bonwon Koo,¹ and Sangyun Lee¹

¹Display Device and Processing Laboratory, Samsung Advanced Institute of Technology, Yongin 446-712, Republic of Korea

²Department of Physics, Dankook University, San 29 Anseo-Dong, Cheonan 330-714, Republic of Korea

³Department of Materials Science and Engineering, Dankook University, San 29 Anseo-Dong, Cheonan 330-714, Republic of Korea

(Received 30 December 2009; accepted 8 April 2010; published online 14 May 2010)

The threshold voltage instability (V_{th}) in indium-gallium-zinc oxide thin film transistor was investigated with disparate SiN_x gate insulators under bias-temperature-illumination stress. As SiN_x film stress became more tensile, the negative shift in V_{th} decreased significantly from -14.34 to -6.37 V. The compressive films exhibit a nitrogen-rich phase, higher hydrogen contents, and higher N–H bonds than tensile films. This suggests that the higher N–H related traps may play a dominant role in the degradation of the devices, which may provide and/or generate charge trapping sites in interfaces and/or SiN_x insulators. It is anticipated that the appropriate optimization of gate insulator properties will help to improve device reliability. © 2010 American Institute of Physics.

[doi:10.1063/1.3429588]

ZnO-based semiconductor thin film transistors (TFTs) are promising candidate that can be incorporated in a variety of electronic applications, such as large area display panels (active matrix liquid crystal displays (AMLCDs) and organic light-emitting diodes). The major attractive aspects are the possibility of fabricating devices at relatively low temperatures and realistic production costs.^{1,2} Intensive researches have been carried out up to date on the performance of oxide semiconductor TFTs.^{3–8} Although the electrical performance is acceptable, the poor stability of oxide semiconductor TFTs with respect to bias stress still remains a crucial problem that inhibits the realization of commercial products.

Recently, a number of groups have studied the stability of ZnO-based oxide TFTs under constant gate bias and/or drain current.^{9–14} The devices were observed to exhibit positive shifts in the threshold voltage (V_{th}) under positive gate bias and/or drain current as a function of stress time. The origin of the V_{th} shift has formerly been investigated with various stress experiments, using different oxide semiconductors,^{6–8} passivation layers,¹² environments,¹⁷ and gate insulators.¹³ In addition, many efforts have been made in order to suppress the degradation of TFTs by adopting impermeable passivation layers,^{15,16} robust

semiconductors,^{7,8} stable TFT structures,¹⁴ and suitable gate insulator materials.¹³ However, most of the above studies have been carried out without the presence of external light. In a real working AMLCD panel, the TFT array is exposed to photon radiation emanating from the backlight unit underneath, and the switching TFT spends most of its lifetime experiencing a negative gate bias that maintains the “off” state of the pixel. It is thus important to examine and improve the stability of the device under negative bias stress with the presence of light radiation to simulate real operating conditions.

In this work, the stability of amorphous InGaZnO (a-IGZO) TFTs is investigated with respect to various SiN_x gate insulators under bias-temperature-illumination stress (BTIS). In particular, an attempt is made at correlating the device stability with the gate dielectric's properties such as film stress, optical constants and hydrogen content.

The detailed device schematics and fabrication procedure are described in a former publication.² TFTs were prepared using three different 400 nm thick SiN_x gate insulators grown by plasma enhanced chemical vapor deposition (PECVD) at a substrate temperature 350 °C. The SiN_x deposition conditions and corresponding device properties are

TABLE I. Deposition conditions and resulting properties of the SiN_x films. (SCCM denotes cubic centimeter per minute at STP.)

	Deposition conditions						Device properties		
	Power (W)	SiH ₄ (SCCM)	NH ₃ (SCCM)	N ₂ (SCCM)	Temperature (°C)	Pressure (Torr)	Film stress (MPa)	Mobility (cm ² /V s)	SS (V/dec)
A SiN _x	650	25	125	1000	350	3.5	-1419	2.55	0.38
B SiN _x	650	25	125	1000	350	2	-890	2.74	0.4
C SiN _x	150	25	125	400	350	2.1	+333	2.05	0.39

^{a)}Authors to whom correspondence should be addressed. Electronic addresses: obmanse@korea.com and jinseongpark@dankook.ac.kr. Tel.: 82-41-550-3514. FAX: 82-41-550-3530.

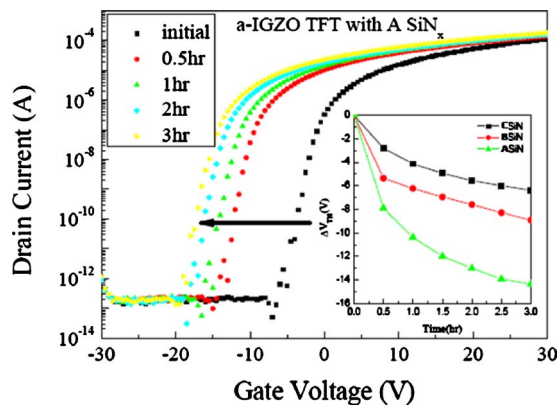


FIG. 1. (Color online) The evolution of the transfer curves for a-IGZO TFTs with A SiN_x gate insulators as a function of the BTIS time ($W/L=90/8$). The variations in the V_{th} shift for A–C SiN_x gate insulators. (inset, values shown in Table I).

listed in Table I. The active a-IGZO film was deposited by radio frequency (rf) magnetron sputtering at room temperature, with thickness 70 nm. After patterning the source-drain electrodes, a 200 nm thick SiO_x passivation layer was grown by PECVD at 150 °C. The electrical characterization of a-IGZO TFTs was carried out using previous conditions²² ($V_{GS}=-20$ V, $V_{DS}=10$ V, substrate temperature of 60 °C, and luminance of 180 lm/m²). In order to examine the gate dielectric properties independently, three different 400 nm thick SiN_x films (named A–C hereafter) were deposited separately onto 4 in. Si (001) wafers. The film stress was measured first, and subsequent vacuum ultraviolet (VUV), spectroscopic ellipsometry (SE), x-ray photoemission spectroscopy (XPS), time-of-flight secondary ion mass spectroscopy (TOF-SIMS), and Fourier transform-infrared (FT-IR) analysis were performed to study the properties of the above SiN_x films.

Figure 1 illustrates the transfer curves that exhibit parallel shifts as a function of the BTIS time. As the stress time increases, the V_{th} shifts in a negative direction without significant variations in the μ_{fe} , SS, and $I_{on/off}$ ratio. In terms of the origin of V_{th} instability, it was suggested in previous reports that simple charge trapping in the gate dielectric and/or at the channel/dielectric interface is dominant compared to the creation of defects within the oxide semiconductor channel.¹² In addition, the insets in Fig. 1 show the negative V_{th} shifts with different SiN_x gate insulators as a function of BTIS times. The film stress values for A, B, and C SiN_x are -1410 MPa (compressive), -890 MPa (compressive), and 333 MPa (tensile), respectively (Table I). The amount of V_{th} shift with the tensile C SiN_x film is smaller than that with the compressive A and B SiN_x dielectrics. One may thus conjecture that the device stability may be closely related to the properties of the SiN_x films, as more compressive gate insulators are accompanied with larger V_{th} shifts.

The density and composition of thin films are reported to be related with the refractive index (n) by the Lorentz–Lorenz law and Gladstone Dale model.^{17,18} The dielectric function ($\epsilon=\epsilon_1+i\epsilon_2$) is also a function of the refractive index (n) and absorption index (k), the latter being affected by variations in electronic, ionic, and space charge polarization.¹⁹ Because the above parameters may have an important influence on the properties of the SiN_x insulators. VUV and SE measurements were performed in the energy

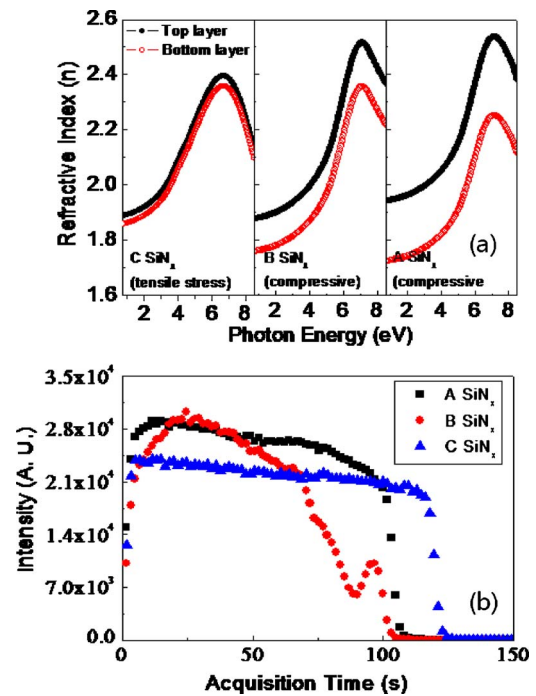


FIG. 2. (Color online) (a) Refractive index values of SiN_x films with tensile and compressive stress with respect to film depth, (b) TOF-SIMS depth profiles for A–C SiN_x gate insulators.

range from 0.75 to 8.5 eV with incident angles of 50°, 60°, and 70°. The refractive index (n) and dielectric function (ϵ) were carefully extracted by the Tauc Lorentz model with multilayer structure comprised of graded layers. Figure 2(a) shows the refractive index measurement results for SiN_x films with tensile and compressive stress, respectively. Each set of data includes the refractive index of the top and bottom layers in accordance with the graded multilayer model in the direction of film depth. The SiN_x films with tensile stress exhibit a uniform distribution of refractive index throughout the entire film, unlike those under compressive stress. Moreover, larger average refractive index values of the top and bottom layer were obtained for tensile SiN_x films, of which the difference is $\sim 0.07 \pm 0.01$. As a result of comparison, higher n values for tensile SiN_x imply higher film density and uniform distribution of dielectric properties along the thickness. The density is higher by approximately 0.4 g/cm³ in the tensile films than the compressive ones, which is calculated by the Gladstone–Dale model based on the difference in refractive index. It is also good agreement with the result of XPS (not shown here), showing that N/Si ratios in tensile and compressive films are 1.13 and 1.3, respectively. In addition, as shown in Fig. 2(b), TOF-SIMS measurements show that the compressive SiN_x films have higher hydrogen contents throughout the entire thickness range. Usually, the SiN_x films with higher silicon-rich and lower hydrogen exhibit higher refractive index and tensile stress behavior like previous reports.^{20,21} At this point it is speculated that these optical and compositional characteristics of SiN_x films may be accompanied with different trapping and detrapping characteristics at the interfacial region between the active a-IGZO and SiN_x gate insulator.

Figure 3 shows the FT-IR spectra, with significant differences in the three SiN_x films, to investigate the hydrogen bonding states. The compressive SiN_x films (A and B) ex

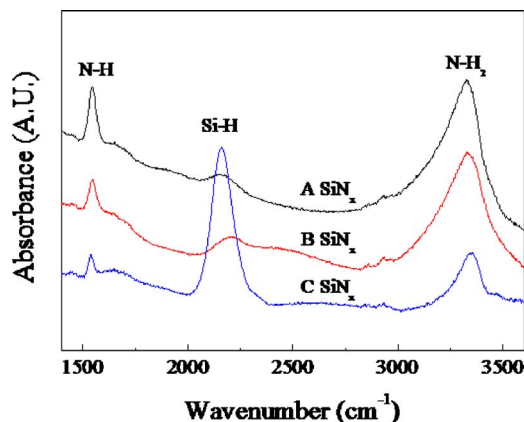


FIG. 3. (Color online) FT-IR adsorption spectra for A–C SiN_x gate insulators.

hibit smaller Si–H absorption peaks and higher N–H and NH_2 absorption intensities than tensile films. As the SiN_x films become more compressive, the overall N–H related absorption intensity increases. It is thus speculated that most of the hydrogen form N–H bonds in compressive SiN_x films, resulting in poor device stability compared to that with tensile films. This implies that higher N–H bond concentrations may generate large amounts of charge trapping sites in a-IGZO TFTs that incorporate SiN_x gate insulators, which deteriorate the device under BITS conditions.

Recently, it has been suggested a possible explanation of the negative BTIS phenomena in a-IGZO TFTs, that photogeneration of carriers and subsequent temporal charge trapping may be responsible for the enhanced V_{th} negative shift²² because the water molecules supplied by the ambient would generate metastable gap states under moisture ambient. However, in this case, there are no metastable gap states resulting from water related trap sites. On the other hand, like silicon metal-oxide-semiconductor field-effect-transistor (MOSFET),^{23,24} it indicates that photogenerated carriers with positive charge would interact and/or combine with nitrogen and/or nitrogen related hydrogen trap sites because the activation energy of positive charge trapping reaction in Si–H is higher than that in N–H site. Therefore, it would be that the C SiN_x gate insulators (tensile, relatively low hydrogen content) show superior results in the device stabilities, compared to the A and B films (compressive, relatively high hydrogen content).

In the present work, the stability of a-IGZO TFTs fabricated with various SiN_x gate insulators were investigated under BTIS conditions. As the film stress of SiN_x gate insulator becomes more tensile, the amount of negative V_{th} shift drastically decreases from -14.34 to -6.37 . The compressive films display a nitrogen-rich phase and relative high hydrogen contents, which may provide charge trapping sites during negative bias stress. In addition, the compressive SiN_x films also contain relatively high concentrations of hydrogen in the form of N–H bonds, inducing larger negative V_{th} shifts in a-IGZO TFTs under negative BTIS. This suggests that the

nitrogen and/or N–H related traps may play a dominant role in the degradation of the devices, for example by generating positive charge trapping sites. From the above results it is anticipated that the selection and/or optimization of gate insulator properties will help to improve the device reliability in oxide TFTs.

Dr. Jin-Seong Park acknowledges the research funding from the Samsung Advanced Institute of Technology and this work was supported by the collaborative R&D program with technology advanced country “Development of materials and stacked device structure for next generation solar cells, 2009-advanced-B-105” by the Ministry of Knowledge and Economy.

- ¹K. Nomura, H. Ohta, K. Ueda, T. Kamiya, M. Hirano, and H. Hosono, *Science* **300**, 1269 (2003).
- ²J. Y. Kwon, K. S. Son, J. S. Jung, T. S. Kim, M. K. Ryu, K. B. Park, B. W. Yoo, J. W. Kim, Y. G. Lee, K. C. Park, S. Y. Lee, and J. M. Kim, *IEEE Electron Device Lett.* **29**, 1309 (2008).
- ³E. Fortunato, P. Barquinha, A. Pimentel, A. Goncalves, A. Marques, L. Pereira, and R. Martins, *Adv. Mater.* **17**, 590 (2005).
- ⁴J. S. Park, J. K. Jeong, Y. G. Mo, H. D. Kim, and S.-I. Kim, *Appl. Phys. Lett.* **90**, 262106 (2007).
- ⁵J. K. Jeong, J. H. Jeong, H. W. Yang, J. S. Park, Y. G. Mo, and H. D. Kim, *Appl. Phys. Lett.* **91**, 113505 (2007).
- ⁶M. K. Ryu, S. Yang, S. H. K. Park, C. S. Hwang, and J. K. Jeong, *Appl. Phys. Lett.* **95**, 072104 (2009).
- ⁷J. S. Park, K. S. Kim, Y. G. Park, Y. G. Mo, H. D. Kim, and J. K. Jeong, *Adv. Mater.* **21**, 329 (2009).
- ⁸C. J. Kim, S. W. Kim, J. H. Lee, J. S. Park, S. I. Kim, J. C. Park, E. H. Lee, J. C. Lee, Y. S. Park, J. H. Kim, S. T. Shin, and U. I. Chung, *Appl. Phys. Lett.* **95**, 252103 (2009).
- ⁹A. Suresh and J. F. Muth, *Appl. Phys. Lett.* **92**, 033502 (2008).
- ¹⁰P. Görrn, P. Holzer, T. Riedl, W. Kowalsky, J. Wnag, T. Weimann, P. Hinze, and S. Kipp, *Appl. Phys. Lett.* **90**, 063502 (2007).
- ¹¹Y. Vygranenko, K. Wang, and A. Nathan, *Appl. Phys. Lett.* **91**, 263508 (2007).
- ¹²J. K. Jeong, H. W. Yang, J. H. Jeong, Y. G. Mo, and H. D. Kim, *Appl. Phys. Lett.* **93**, 123508 (2008).
- ¹³J. S. Lee, J. S. Park, Y. S. Pyo, D. B. Lee, E. H. Kim, D. Stryakhilev, T. W. Kim, D. U. Jin, and Y. G. Mo, *Appl. Phys. Lett.* **95**, 123502 (2009).
- ¹⁴S. I. Kim, J. S. Park, C. J. Kim, J. C. Park, I. H. Song, and Y. S. Park, *J. Electrochem. Soc.* **156**, H184 (2009).
- ¹⁵D. H. Levy, D. Freeman, S. F. Nelson, P. J. Cowdery-Corvan, and L. M. Irving, *Appl. Phys. Lett.* **92**, 192101 (2008).
- ¹⁶S. E. Thompson, M. Armstrong, C. Auth, S. Cea, R. Chau, G. Glass, T. Hoffman, J. Klaus, Z. Ma, B. McIntyre, A. Murthy, B. Obradovic, L. Shifren, S. Sivakumar, S. Tyagi, T. Ghani, K. Mistry, M. Bohr, and Y. El-Mansy, *IEEE Electron Device Lett.* **25**, 191 (2004).
- ¹⁷K. Ishii, A. Takami, and Y. Ohki, *J. Appl. Phys.* **81**, 1470 (1997).
- ¹⁸J.-H. Kim, C.-O. Chung, D. Sheen, Y.-S. Sohn, H.-C. Sohn, J.-W. Kim, and S.-W. Park, *J. Appl. Phys.* **96**, 1435 (2004).
- ¹⁹S.-W. Chung, J.-H. Shin, N.-H. Park, and J. W. Park, *Jpn. J. Appl. Phys.* **38**, 5214 (1999).
- ²⁰M. Belyansky, M. Chace, O. Gluschenkov, J. Kempisty, N. Klymko, A. Madan, A. Mallkarjunan, S. Molis, P. Ronsheim, Y. Wang, D. Yang, and Y. Li, *J. Vac. Sci. Technol. A* **26**, 517 (2008).
- ²¹A. K. Stamper and S. L. Pennigton, *J. Electrochem. Soc.* **140**, 1748 (1993).
- ²²K.-H. Lee, J. S. Jung, K. S. Son, J. S. Park, T. S. Kim, R. Choi, J. K. Jeong, J. Y. Kwon, B. Koo, and S. Y. Lee, *Appl. Phys. Lett.* **95**, 232106 (2009).
- ²³D. K. Schroder and J. A. Babcock, *J. Appl. Phys.* **94**, 1 (2003).
- ²⁴K. Kushida-Abdelghafar, K. Watanabe, J. Ushio, and E. Murakami, *Appl. Phys. Lett.* **81**, 4362 (2002).